Soft Matter

PAPER

View Article Online
View Journal | View Issue

Cite this: *Soft Matter*, 2014, **10**, 2632

Insights into organogelation and its kinetics from Hansen solubility parameters. Toward *a priori* predictions of molecular gelation†

Kevin K. Diehn,[a] Hyuntaek Oh,[a] Reza Hashemipour,[a] Richard G. Weiss[b] and Srinivasa R. Raghavan*[a]

Received 30th August 2013
Accepted 3rd February 2014

DOI: 10.1039/c3sm52297k

www.rsc.org/softmatter

Many small molecules can self-assemble by non-covalent interactions into fibrous networks and thereby induce gelation of organic liquids. However, no capability currently exists to predict whether a molecule in a given solvent will form a gel, a low-viscosity solution (sol), or an insoluble precipitate. Gelation has been recognized as a phenomenon that reflects a balance between solubility and insolubility; however, the distinction between these regimes has not been quantified in a systematic fashion. In this work, we focus on a well-known gelator, 1,3:2,4-dibenzylidene sorbitol (DBS), and study its self-assembly in various solvents. From these data, we build a framework for DBS gelation based on Hansen solubility parameters (HSPs). While the HSPs for DBS are not known *a priori*, the HSPs are available for each solvent and they quantify the solvent's ability to interact *via* dispersion, dipole–dipole, and hydrogen bonding interactions. Using the three HSPs, we construct three-dimensional plots showing regions of solubility (S), slow gelation (SG), instant gelation (IG), and insolubility (I) for DBS in the different solvents at a given temperature and concentration. Our principal finding is that the above regions radiate out as concentric shells: *i.e.*, a central solubility (S) sphere, followed in order by spheres corresponding to SG, IG, and I regions. The distance (R_0) from the origin of the central sphere quantifies the incompatibility between DBS and a solvent—the larger this distance, the more incompatible the pair. The elastic modulus of the final gel increases with R_0, while the time required for a super-saturated sol to form a gel decreases with R_0. Importantly, if R_0 is too small, the gels are weak, but if R_0 is too large, insolubility occurs—thus, strong gels fall within an optimal window of incompatibility between the gelator and the solvent. Our approach can be used to design organogels of desired strength and gelation time by judicious choice of a particular solvent or a blend of solvents. The above framework can be readily extended to many other gelators, including those with molecular structures very different from that of DBS. We have developed a MATLAB program that will be freely available (upon request) to the scientific community to replicate and extend this approach to other gelators of interest.

Introduction

Molecular organogels are a fascinating class of materials that are attracting wide interest among chemists, physicists and engineers.[1–3] They are formed by the non-covalent self-assembly of small molecules in organic liquids. The molecular assembly results in long one-dimensional objects ("fibers"), which entangle and interconnect into a three-dimensional (3-D) network.[4] Upon formation of such a self-assembled fibrous network (SAFIN), the liquid solvent (sol) is entrapped within the network, and the sample is transformed into an elastic gel. Molecular organogels are being explored for a variety of applications such as for treating oil spills,[5] art conservation,[6] plasma and serum separation,[7] and as functional materials in solar cells or lithium-ion batteries.[8]

Despite the wide interest in molecular gels, a fundamental understanding of self-assembly-based gelation is lacking. Most known organogelators have been discovered by serendipity, and trial-and-error experiments are still necessary to determine which solvents they can gel.[2,9,10] It would be invaluable to have a framework that could be used to predict whether a given gelator could gel a new solvent of interest. For various solvents, important physical properties such as the dielectric constant, Hamaker constant, surface tension, Hildebrandt solubility parameter, and Hansen solubility parameters, are either tabulated or can be calculated. Can gelation be correlated with one

[a]*Dept. of Chemical & Biomolecular Engineering, University of Maryland, College Park, MD 20742-2111, USA. E-mail: sraghava@umd.edu*

[b]*Dept. of Chemistry & Institute of Soft Matter Synthesis & Metrology, Georgetown University, Washington, DC 20057-1227, USA*

† Electronic supplementary information (ESI) available: The experimental section, a section on fitting procedures, and additional tables and figures. See DOI: 10.1039/c3sm52297k

or more of these physical properties? This question has generated much research,[11–15] but the field still awaits a framework that has applicability across a wide range of molecular gelators.

An important advance in connecting gelation with solvent properties was recently reported by Raynal and Bouteiller[16] who performed a meta-analysis of eight earlier studies on organogelators. They interpreted these results in terms of the solvents' Hansen solubility parameters (HSPs).[17,18] The same approach has also been subsequently used by other researchers.[19–23] HSPs quantify the cohesive energy density δ of a solvent in terms of contributions from three types of weak interactions:[17] van der Waals or dispersive interactions (δ_D), dipole–dipole or polar interactions (δ_P), and hydrogen-bonding interactions (δ_H). Each solvent is thus a point on a 3-D plot in which the axes represent the three HSPs (δ_D, δ_P, and δ_H). The distance from the origin to that point represents the total cohesive energy density δ of the solvent.[17] In the present study, we develop a new HSP-based framework for interpreting gelation that offers important insights and useful predictive capabilities.

The focus of our studies is the well-known model organogelator 1,3:2,4-dibenzylidene sorbitol (DBS). DBS is a butterfly-shaped molecule with a hydroxylated center and benzyl groups on either side (Fig. 1) and it is capable of gelling many organic solvents at low concentrations (<5 wt%).[21,24–31] We examine DBS in a wide range of solvents with known HSPs and we plot our observations on 3-D Hansen plots. (Note that the precise HSPs of DBS are not known *a priori*. Group contribution methods do exist to determine HSPs from the functional groups present in a given molecule;[17,21] however, these can be reliably applied only to simple molecules, not to complex structures like DBS.) Our central finding is a consistent, logical progression in 3-D Hansen space with spherical shells of solubility, gelation, and insolubility radiating out in order. This pattern offers insights into both the nature and the kinetics of gelation. In addition, we are also able to correlate the rheology of DBS gels with the solvent properties based on HSPs.

Results and discussion

Procedure and classification of outcomes

The HSPs for hundreds of neat organic solvents are collected in the book by Hansen.[17] We studied DBS in many of these solvents, with some candidate solvents identified from the previous literature.[21,25–31] Our procedure employed visual observation of DBS-solvent mixtures and is schematically depicted in the left panel of Fig. 1. First, DBS was added to the solvent at a desired concentration and the mixture was heated to 125 °C while being stirred. This typically resulted in a low-viscosity, transparent solution (sol). The vial containing the hot sol was then cooled to room temperature using running water (22 °C) for 90 s. From this point onwards, the vial was placed on the countertop and observed visually. Vial inversion was used to infer the formation of an organogel, *i.e.*, a sample was termed a gel if it held its own weight in the inverted vial.[32]

Sample outcomes were categorized in the following manner. A sample was classified to be insoluble (**I**) if: (a) DBS could not be dissolved even after heating and stirring, or (b) it was soluble at high temperature (T) but formed a solid precipitate upon

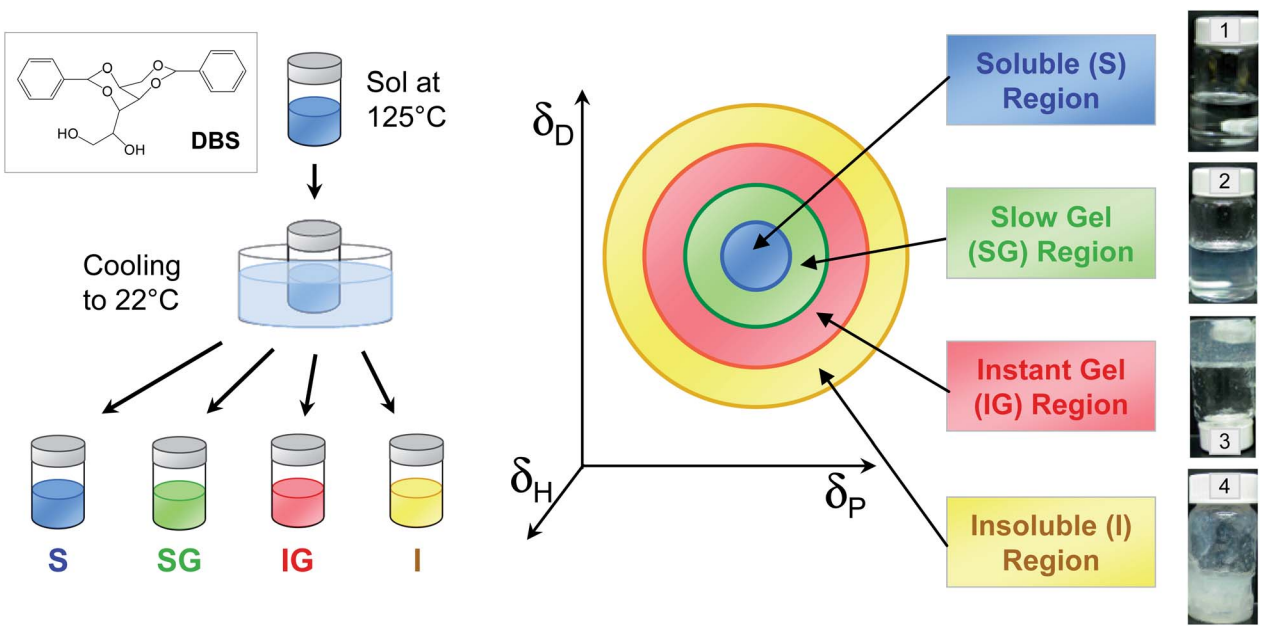

Fig. 1 **Schematic of the experimental setup (left) and the corresponding results in 3-D Hansen space (right).** The organogelator DBS was added to various organic solvents and heated to 125 °C, followed by cooling to room temperature (22 °C). Visual observations were used to classify the samples as soluble or sols (**S**, blue), slow gels (**SG**, green), instant gels (**IG**, red) and insoluble (**I**, yellow). Photographs of samples corresponding to these outcomes are shown on the right. These outcomes were then plotted for the various solvents on a 3-D plot where the axes represent the three Hansen solubility parameters (δ_D = dispersive, δ_P = polar, and δ_H = hydrogen-bonding interactions). Our key finding, shown by the schematic figure on the right, is that the four regions radiate out as concentric shells: *i.e.*, the central sol (**S**) sphere, followed in order by **SG**, **IG**, and **I** spheres.

cooling to room temperature. Photo 4 in Fig. 1 is an example of such a sample. Next, a sample was classified as a sol or solution (**S**) if it remained a thin, clear liquid indefinitely after cooling to room temperature (photo 1). That is, sols remained so regardless of time; they did not subsequently convert into gels or become unstable and precipitate. Next, concerning the samples that did transform from sols at high T to gels at ambient temperature, we further distinguished two cases depending on the relative kinetics of gelation. If the sample was already a gel (as indicated by vial inversion) by the time it was cooled to room temperature (time $t = 0$), it was classified as an instant gel (**IG**). On the other hand, if the sample was not a gel at $t = 0$ but it formed a gel at some finite time t_{gel} after reaching room temperature, it was classified as a slow gel (**SG**) and the corresponding t_{gel} was recorded. The distinction between **IG** and **SG**, although qualitative, is important because gelation is usually a non-equilibrium process and there is a kinetic aspect to it.[2,33] For example, many gels, including those of DBS, form by the nucleation and growth of fibrils. Thus, a simple either-or approach to gelation (*i.e.*, gel or no gel) could produce different results depending on the procedure employed and the time at which the sample is observed. The use of the four-pronged **S–SG–IG–I** scheme mitigates against these issues.

Plotting outcomes in 3-D Hansen space

To visualize the regions of DBS outcomes, each solvent was plotted as a point in 3-D Hansen space where each axis represents one of the HSPs (δ_D, δ_P, δ_H). The solvent points were color-coded based on the outcome of the sample, with blue for soluble (**S**), green for slow gel (**SG**), red for instant gel (**IG**), and yellow for insoluble (**I**). Next, color-coded spheres were drawn around each of these regions on the 3-D plot. The use of spherical regions mirrors the method used by Hansen for polymer–solvent interactions.[17,18] In our approach, we have made a few critical choices that depart from previous work on HSP-gelator correlations. First, we begin by focusing on the blue sphere corresponding to the soluble (**S**) region in Fig. 1. The criterion for this sphere is that it must encompass all the solvents in which DBS gives a sol (the "good" solvents) while excluding all other solvents (the "bad" solvents). The size of the **S** sphere (*i.e.*, its radius R_S) and its location (*i.e.*, its origin in 3-D space) are the two variables. We used a MATLAB program to find the location and size of the optimal **S** sphere that satisfied the above criterion. The algorithm and fitting procedure are discussed in Section 2 of the ESI† and screenshots of the program are shown in Fig. S1.† Briefly, we make an initial guess for the location of the origin and an initial value of the radius based on our data. Taking cues from Hansen's work, we employ a desirability function (DF) to determine the goodness-of-fit for this radius and origin (see Section 2, ESI†).[17,18] We then iterate the location and size of the S sphere until the DF is maximized.

Once the soluble (**S**) sphere is correctly sized and placed, *we then use the same origin for the subsequent **SG, IG and I** spheres*. This is a crucial distinction from previous studies and we believe it leads to a simpler and more intuitive framework. The resulting plots are shown schematically in Fig. 1. Considering the **SG** (green) sphere, we fix its origin as that of the **S** (blue) sphere and iterate its radius R_{SG} such that it encompasses the solvents in which DBS forms a slow gel while excluding the solvents corresponding to the **IG** and **I** outcomes. Similarly, we draw the **IG** (red) sphere under the criterion that it includes the solvents in which DBS forms an instant gel while excluding the solvents in which DBS is insoluble. Finally, we plot the **I** (yellow) sphere by extending it up to the solvent points corresponding to DBS insolubility. Our central result is that the four regions radiate out as concentric shells (Fig. 1): *i.e.*, the central soluble (**S**) sphere is followed in order by spheres corresponding to the **SG**, **IG**, and **I** regions. We will discuss the implications of this result after first presenting the actual data.

3-D plots for DBS

DBS sample outcomes were determined and plotted by the above procedure for three DBS concentrations: 1%, 5% and 10% (weight/volume). A total of 35 solvents were tested and their HSPs are provided in Table S1 that is part of the ESI file.† The plots in 3-D Hansen space are shown in Fig. 2. Note also that these results pertain to room temperature (~22 °C). For convenient representation, the vertical axis is not extended to the origin and its values correspond to $2\delta_D$; the other two axes correspond to δ_P and δ_H. The use of $2\delta_D$ is per the recommendation of Hansen as it is conducive to spherical fits.[17,18]

The plots in Fig. 2 clearly reveal the key result mentioned above, which is the presence of a central solubility (**S**) sphere in blue followed by radiating spherical shells corresponding to **SG** (green), **IG** (red) and **I** (yellow) regions. The concentric spheres reflect our analysis procedure, but they are derived from the empirical observations. To emphasize this aspect, we show the empirical outcomes in the various solvents as discrete color-coded points. Enlarged versions of these three plots are provided in the ESI (Fig. S2†). Note that the blue points are clustered in the center of the blue (**S**) sphere and as one moves radially outward, a number of green (**SG**) points appear, then several red (**IG**) points and finally some yellow (**I**) points. (As an aside, viewing the 3-D plots in 2-D can sometimes be misleading; *i.e.*, points that appear to be inside a given sphere may actually be outside it.) The underlying result in terms of a progression in Hansen space from solubility to gel to insoluble is in accord with the seminal paper by Raynal and Bouteiller,[16] although they did not separate out the **SG** and **IG** regions.

Several trends are evident from the plots in Fig. 2. First, note that the blue sol (**S**) sphere is relatively large at 1% DBS (Fig. 2a) and then shrinks to a constant size as the DBS concentration is increased to 5 and 10% (Fig. 2b and c). This result reveals the concentration-dependent nature of molecular gelation: *i.e.*, samples that are sols at low gelator concentrations may become gels at higher gelator concentrations. Note also that the origin of the **S** sphere in the three above plots has a nearly constant location. The co-ordinates of the origin in terms of HSPs (δ_{D°, δ_{P°, δ_{H°) are (17.8, 13.6, 6.4) for 1% DBS, (17.6, 15.7, 9.3) for 5% DBS and (17.6, 15.7, 9.3) for 10% DBS (all numbers have units of $MPa^{1/2}$). The origin of the **S** sphere is significant because it provides an estimate for the HSPs of DBS itself. Interestingly,

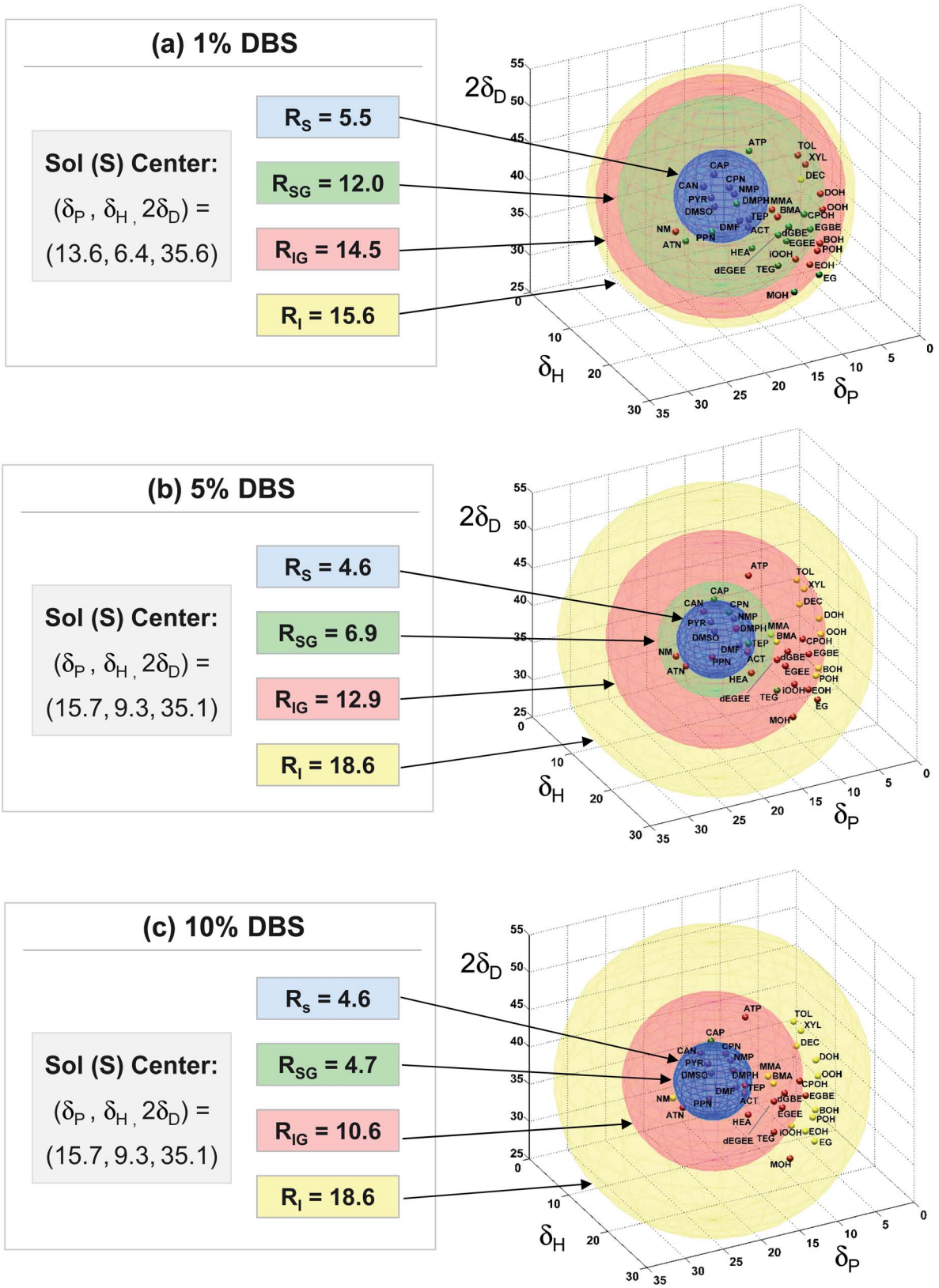

Fig. 2 **Results for DBS in various solvents, plotted in 3-D Hansen space: (a) 1%; (b) 5%; and (c) 10% DBS.** The axes represent the three Hansen solubility parameters (δ_D = dispersive, δ_P = polar, and δ_H = hydrogen-bonding interactions). Each solvent is represented as a color-coded point on these plots. The results show a pattern of concentric spheres, *i.e.*, the central sol (**S**) sphere in blue, followed in order by spheres corresponding to slow gel (**SG**) in green, instant gel (**IG**) in red, and insoluble (**I**) in yellow. The co-ordinates for the center of the **S** sphere and the radii of each sphere are indicated. Enlarged versions of the same plots are provided in Fig. S2 (ESI).†

however, the above estimates are quite different from a recent calculation of the HSPs of DBS by a group contribution method, which determined (δ_{D°, δ_{P°, δ_{H°) to be (15.9, 3.9, 18.3) (again in $MPa^{1/2}$).[21] We believe this discrepancy indicates the difficulty of using group contribution methods to calculate HSPs for complex molecules. Note that the HSPs of DBS are expected to be close to those of the solvents in which it is most soluble. Empirically, we find that DBS is highly soluble (even at 10%) in polar aprotic solvents such as *N*-methylpyrrolidone (NMP), dimethylsulfoxide (DMSO), and dimethylformamide (DMF). All these solvents fall near the center of the S sphere and in turn, their HSPs are close to the values for the origin.

Next, we discuss trends in the **SG**, **IG** and **I** regions. At a low concentration (1%) of DBS, many gels form slowly after cooling and therefore the green **SG** region is large. Correspondingly, only few solvents reveal a gel as soon as the sample is cooled, and thus the red **IG** region is just a thin shell. As DBS is increased to 5%, the **SG** region shrinks while the **IG** region substantially expands. Finally, at 10% DBS, the **SG** region is a very thin, almost non-existent shell surrounding the **S** sphere and most of the gels are instant gels, falling in the **IG** region. In other words, when the concentration of gelator is high, gels form rapidly regardless of solvent. Note also that the boundary of the **IG** region, *i.e.*, the radius R_{IG} of the sphere, shrinks with increasing DBS. This means that some solvents are unable to completely solubilize high concentrations of DBS, which leads to a classification of these samples as insoluble (**I**). In turn, the **I** region expands with increasing DBS.

We will now mention a few trends regarding the chemical nature of the solvents tested and its impact on DBS gelation. As mentioned, DBS is highly soluble and non-gelling in polar aprotic solvents like NMP[25] and DMF. Conversely, in non-polar aliphatic liquids like *n*-alkanes, DBS is insoluble, as noted by previous studies.[21] DBS forms strong, instant gels even at low concentrations in aromatic solvents such as toluene and xylene, as well as in short-chain alcohols like 1-propanol and 1-butanol. In diols such as ethylene glycol as well as in glycol ethers, DBS shows slow gelation at low concentrations and instant gelation at higher concentrations. Based on these findings, DBS gelation appears to be a complex process mediated by several weak interactions, which may include van der Waals, H-bonding, and possibly π–π stacking.[29] One cannot attribute the gelation ability of DBS simply to H-bonding[26] even though the molecule has two primary –OH groups. Indeed, DBS is able to gel solvents like the diols, which also have –OH groups that can compete for H-bonding.

Significance of the S–SG–IG–I concentric shells

The 3-D plots for DBS shown in Fig. 2 and illustrated in Fig. 1 provide a logical framework for gelation. Researchers have recognized that gelation requires a balance between solubility and insolubility.[1–3] If a gelator is too soluble in a solvent (*i.e.*, if it is too similar or compatible with the solvent), a sol is formed. The HSPs allow us to quantify this intermolecular similarity. That is, if the HSPs of the gelator and a solvent are nearly equal, then the mixture will fall in the solubility (**S**) sphere and will correspond to a sol.[16,19] In the other extreme, if the gelator and solvent are too incompatible, *i.e.*, if their HSPs are widely different, the gelator will be insoluble and the sample will fall in the **I** region. The incompatibility between solvent and gelator is proportional to the distance R_0 in 3-D space from the solvent point to the origin of the **S** sphere.[17] When R_0 is small such that $R_0 < R_S$, it corresponds to the soluble (**S**) region and when R_0 is large such that $R_0 > R_{IG}$, it corresponds to the **I** region. Note that R_0 can be calculated for a given solvent j (of known HSPs) if we know the HSPs at the origin of the **S** sphere (eqn (1)):[17]

$$R_0 = \sqrt{4\left(\delta_D^j - \delta_{D^\circ}\right)^2 + \left(\delta_P^j - \delta_{P^\circ}\right)^2 + \left(\delta_H^j - \delta_{H^\circ}\right)^2} \qquad (1)$$

Between the above extremes, if the gelator is in a solvent that is moderately incompatible ($R_S < R_0 < R_{IG}$), it forms a gel. Moreover, if the HSPs of a solvent are such that it falls just outside the sol (**S**) sphere (*i.e.*, if $R_S \approx R_0$), then the gelator forms a slow gel (**SG**) in this solvent, at least at low gelator concentrations. On the other hand, if the HSPs of the solvent place it far from the **S** sphere and close to the **I** boundary (*i.e.*, if $R_S \ll R_0 \approx R_{IG}$), the gelator forms an instant gel (**IG**) in this solvent even at low concentrations. There is a continuum between the **SG** and **IG** regions: increasing the gelator concentration causes the **SG** region to shrink and the **IG** region to expand. Conversely, the reverse (expansion of **SG**, shrinking of **IG**) is expected on increasing temperature.

Gel properties as a function of R_0

The above analysis implies a systematic variation in gel properties with the distance R_0 from the center of the **S** sphere. That is, gels near the **S** boundary should take longer to form and should be weaker than those that are farther away from this boundary. To test these predictions, we have measured the elastic modulus G' from dynamic rheology for 5% DBS in a variety of solvents corresponding to the **SG** and **IG** regions. Fig. 3 plots G' *vs.* the R_0 of the solvent. Note that the R_0 axis is on

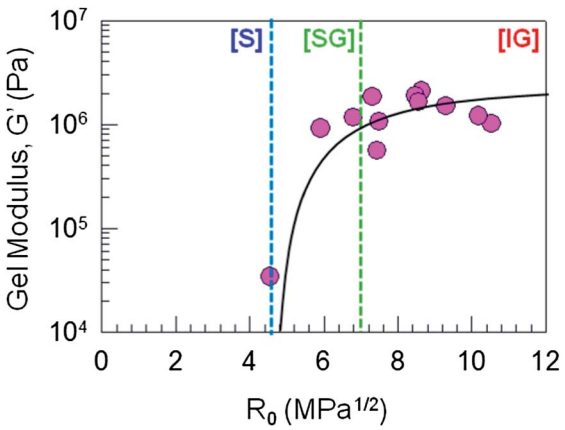

Fig. 3 Correlation of gel modulus with Hansen parameters. The elastic modulus G' of 5% DBS gels in various solvents is plotted as a function of the distance R_0 of the corresponding solvent from the center of the solubility (S) sphere in Fig. 2b. The values of R_0 at the boundaries of the S and SG regions are shown for reference. The data reveal an increasing trend in G' with R_0. The line is drawn to guide the eye.

a linear scale while the G' axis is on a log scale. We confirmed that all the samples showed the signature of gels:[4,32] *i.e.*, in frequency sweeps, both the elastic modulus G' and the viscous modulus G'' were independent of frequency and G' exceeded G''. (In the case of the slow gels, we measured the rheology well after the gelation was complete.) For reference, the values of R_0 at the boundaries of the **S** and **SG** regions are indicated in Fig. 3. The plot does show an increasing trend in gel modulus G' with increasing R_0, indicating that gels farther from the **S** boundary are stiffer. The trend is not perfect and many slow gels have moduli that are comparable to those of the instant gels. The slow gel that lies closest to the **S** boundary has the lowest G'. We should mention that G' does exhibit a more systematic dependence on R_0 than on the differences between any of the individual HSPs (δ_D, δ_P, δ_H), as shown in Fig. S3 (ESI).†

Next, we explored the relationship between gelation time t_{gel} and R_0, and this is presented in Fig. 4. These measurements were done in various solvents corresponding to the **SG** and **IG** regions for 5% DBS. Again, note that the t_{gel} axis is on a log scale while the R_0 axis is on a linear scale. For the instant gels, we have arbitrarily designated a low value of $t_{gel} = 10^{-1}$ min. The plot shows a decreasing trend in t_{gel} with increasing R_0 within the **SG** region. Again, this trend is not perfect and moreover, the distinction between slow and instant gel regions is not always clear-cut. Nevertheless, the limiting behavior is revealed by this plot. That is, at the edge of the soluble (**S**) region ($R_0 = 4.6$), $t_{gel} \rightarrow \infty$ as the favorable solvent–gelator interactions strongly interfere with the assembly of fibers. As the distance from the **S** region increases, t_{gel} decreases and, at the other extreme, the plot reaches a plateau at $t_{gel} \rightarrow 0$ in the **IG** region.

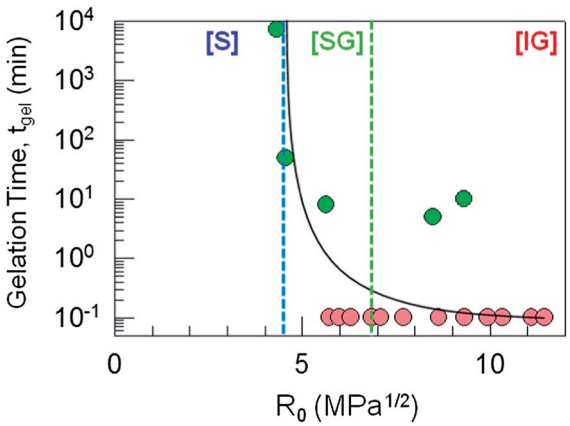

Fig. 4 **Correlation of gelation time with Hansen parameters.** For the case of 5% DBS gels in various solvents, the time to form a gel after cooling to room temperature (t_{gel}) is plotted as a function of the distance R_0 of the corresponding solvent from the center of the solubility (S) sphere in Fig. 2b. For each of the instant gel (IG) points (red circles), a gelation time of 10^{-1} min is arbitrarily assigned. The slow gel (SG) points are shown as green circles. Note that some SG points occur in the IG region and *vice versa*; this is unavoidable with the fitting algorithm employed. The values of R_0 at the boundaries of the S and SG regions are shown for reference. At the boundary of the S region, t_{gel} diverges. As one moves away from this boundary, t_{gel} tends to decrease with increasing R_0. The curve is drawn to guide the eye.

Prediction of gelator behavior in solvent mixtures

Based on the above analysis, we can offer a few predictions and test them. For example, consider mixtures of two miscible solvents with known HSPs. The HSPs of the mixtures can be estimated by linear interpolation based on the HSPs of the pure solvents and their volume fractions (assuming ideal mixing).[17] On the 3-D plot, this corresponds to straight lines between the two solvent points. Can the outcomes for DBS in such mixtures be predicted based on the locations of the mixture points on the 3-D plot?

To test this, we have considered DMSO as one of the solvent components of the mixture. DBS is highly soluble in DMSO and thus its point occurs in the middle of the **S** region (Fig. 5). We then considered five solvents as the second component of the mixture: 1-decanol, 1-octanol, 1-butanol, ethylene glycol, and toluene. These solvent points fall in the **I** or **IG** regions. We examined 5% DBS in blends of DMSO with these five solvents. The points corresponding to these mixtures fall along five lines on the 3-D plot, as shown in Fig. 5, and the color-coded empirical outcomes for each of these mixtures is indicated. A different view of the same data is shown in Fig. S4 (ESI).† For each solvent pair, we see a progression from sols (blue points) in DMSO to slow gels (green points) to instant gels (red points). For the three 1-alkanols and toluene, insolubility (yellow points) occurs at high volume fractions. Note that the blue points fall a bit outside the solubility (**S**) sphere determined previously for neat solvents; however, the correct trend is seen in all cases. The differences may be related to non-ideal mixing of the solvents or to selective solvation of DBS. We can conclude from Fig. 5 that our analysis based on HSPs has reasonably good predictive power: for a given gelator, once the center of the **S** sphere and the radii of the **S**, **SG** and **IG** spheres are determined, the behavior of the gelator in an untested solvent can be predicted to a first approximation based only on the solvent's HSP values.[22,23]

One adaptation of the above approach has been reported in a recent study co-authored by some of us involving pyrenyl-linker-glucono gelators.[23] The unusual result in this study was that a gelator was insoluble in two neat solvents, tetrahydrofuran (THF) and water, but it formed a gel in THF-water mixtures.[23] How to explain this result? The logic behind this is indicated in Fig. S5 (ESI†): if the gelator is insoluble (**I**) in two solvents that fall on either side of the solubility (**S**) sphere, then a line drawn between the two solvents can cut through the **S**, **SG** and **IG** regions. For example, taking the case of DBS, two such solvents could be nitromethane and 1-octanol. Depending on the ratio of these two solvents, DBS samples are predicted based on Fig. S5† to range from sols to slow gels to instant gels.

Thumb rules and outlook

In terms of thumb rules (independent of concentration) for the distance R_0 from the center of the **S** sphere, we estimate that $R_0 < 5$ MPa$^{1/2}$ results in solubility; $R_0 \sim 10$ MPa$^{1/2}$ results in gelation; and $R_0 \sim 15$ MPa$^{1/2}$ results in insolubility. It will be interesting to apply this analysis to other gelators and to test the validity of the above thumb rules. Note that all three HSPs need

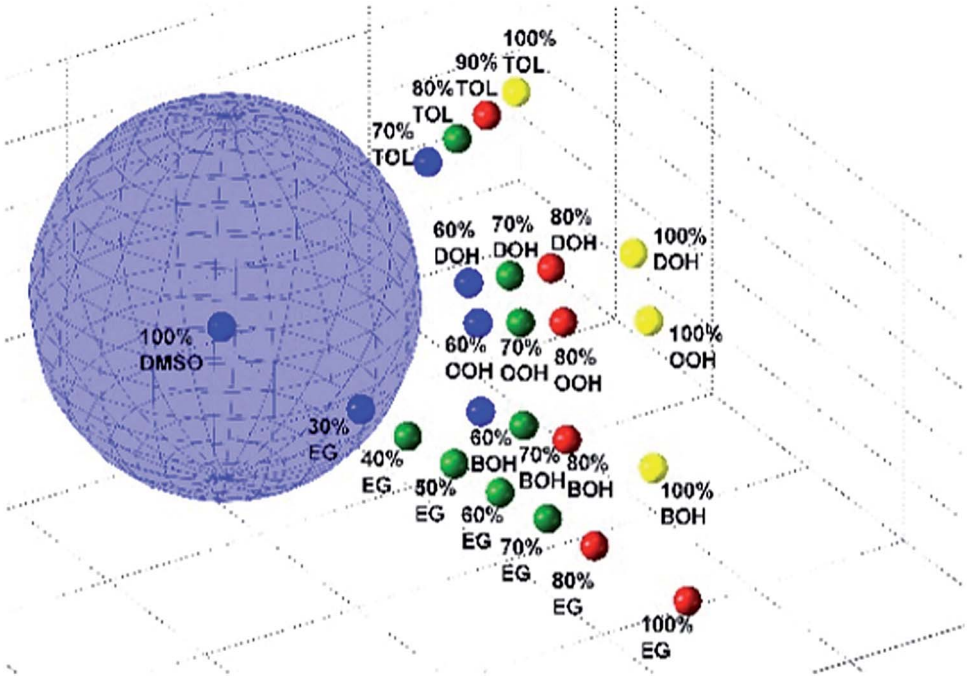

Fig. 5 **Outcomes for DBS in solvent blends, plotted in 3-D Hansen space.** DBS was studied at a concentration of 5% in mixtures of DMSO and the following solvents: toluene (TOL), 1-decanol (DOH), 1-octanol (OOH), 1-butanol (BOH) and ethylene glycol (EG). On the Hansen plot, solvent mixtures fall on straight lines between the points corresponding to the individual solvents, as shown above. DBS is highly soluble in DMSO, and the pure DMSO point is near the center of the solubility (**S**) sphere (this sphere is identical to that in Fig. 2b). For the mixtures, the sample outcomes are color coded as: sols (**S**, blue), slow gels (**SG**, green), instant gels (**IG**, red) and insoluble (**I**, yellow). A systematic progression in sample outcomes is seen for all the solvent pairs. A top view of the above plot (along the $\delta_P-\delta_H$ plane) is shown in Fig. S4 (ESI).†

to be used to calculate R_0 by eqn (1). That is, the difference in total cohesive energy density between gelator and solvent is what is predicted to dictate gelation behavior.

To facilitate the application of our approach to other gelators, we have developed a **standalone program and graphical user interface** (based on underlying MATLAB code) that will be made available on the Internet at no cost (upon request). Our program enables a user to input data for their gelator of interest in different solvents in the form of a Microsoft Excel spreadsheet. The spreadsheet has to adhere to a set template, which includes a list of solvents with their HSPs and the outcomes with the gelator (sol, slow gel, instant gel, insoluble) for each case. The program then generates 3-D Hansen plots similar to those shown in Fig. 2. Screenshots of the program are shown in Fig. S1 (ESI).† Two modes of fitting are offered. In one mode, the user may fit the regions as shells radiating from a central solubility sphere, as was done in Fig. 2. In the other mode, the user may fit the regions as discrete spheres in Hansen space. The program calculates the centers and radii of the spheres corresponding to optimal goodness-of-fit values. Our method enables simple benchtop data on gelators to be visualized and analyzed for insights.

We should note that the approach of fitting concentric spheres with the same center point is clearly the simplest and most intuitive approach, but it remains to be seen whether this would apply to gelators with more complicated molecular structures. For example, gelators with large, well-separated hydrophobic and hydrophilic parts could be solvated inhomogeneously in different solvents as well as in solvent mixtures. In such cases, there will be a need for refinement of the approach presented here. Sacrificing the simplicity of the approach for better predictability will be a decision that must be made by each scientist for their gelators of interest. In the future, it is possible to modify and expand the above MATLAB program to account for various types of complications that occur for specific gelators.

Conclusions

We have applied a simple methodology to characterize systematically the self-assembly of a model organogelator DBS in a number of organic solvents. Gelator behavior was classified initially by benchtop experiments and the various outcomes were placed on 3-D plots where the axes correspond to the three Hansen solubility parameters (HSPs). The results follow a pattern of concentric spheres with a central solubility (**S**) sphere surrounded by spherical regions corresponding to slow gelation (**SG**), instant gelation (**IG**), and insolubility (**I**). The pattern suggests that gelation requires a moderate extent of incompatibility between the gelator and solvent. The latter can be quantified by the distance R_0 from the center of the **S** sphere. The modulus of the organogels increases with R_0 while the time to form the gels decreases with R_0. Our approach gives reasonable predictions of gelator behavior in untested solvents, such as solvent blends. Thumb rules based on the above approach can be tested by experiments with other gelators. A

MATLAB program and an associated graphical user interface (GUI) have been developed to allow other researchers to apply the same approach to their gelators.

Acknowledgements

This work was funded by a grant from the National Science Foundation Chemistry Division (CHE-0911089). Helpful discussions with Prof. Partho Dastidar (IACS, India) and Dr Jack Douglas (NIST) are acknowledged.

References

1 *Molecular Gels: Materials with Self-Assembled Fibrillar Networks*, ed. R. G. Weiss and P. Terech, Springer, Dordrecht, 2006.
2 P. Terech and R. G. Weiss, Low molecular mass gelators of organic liquids and the properties of their gels, *Chem. Rev.*, 1997, **97**, 3133–3159.
3 N. M. Sangeetha and U. Maitra, Supramolecular gels: Functions and uses, *Chem. Soc. Rev.*, 2005, **34**, 821–836.
4 S. R. Raghavan and J. F. Douglas, The conundrum of gel formation by molecular nanofibers, wormlike micelles, and filamentous proteins: gelation without cross-links?, *Soft Matter*, 2012, **8**, 8539–8546.
5 S. R. Jadhav, P. K. Vemula, R. Kumar, S. R. Raghavan and G. John, Sugar-derived phase-selective molecular gelators as model solidifiers for oil spills, *Angew. Chem., Int. Ed.*, 2010, **49**, 7695–7698.
6 E. Carretti, M. Bonini, L. Dei, B. H. Berrie, L. V. Angelova, P. Baglioni and R. G. Weiss, New frontiers in materials science for art conservation: Responsive gels and beyond, *Acc. Chem. Res.*, 2010, **43**, 751–760.
7 K. S. Sun, H. Oh, J. F. Emerson and S. R. Raghavan, A new method for centrifugal separation of blood components: Creating a rigid barrier between density-stratified layers using a UV-curable thixotropic gel, *J. Mater. Chem.*, 2012, **22**, 2378–2382.
8 V. R. Basrur, J. C. Guo, C. S. Wang and S. R. Raghavan, Synergistic gelation of silica nanoparticles and a sorbitol-based molecular gelator to yield highly-conductive free-standing gel electrolytes, *ACS Appl. Mater. Interfaces*, 2013, **5**, 262–267.
9 P. Dastidar, Supramolecular gelling agents: Can they be designed?, *Chem. Soc. Rev.*, 2008, **37**, 2699–2715.
10 A. Dawn, T. Shiraki, S. Haraguchi, S. Tamaru and S. Shinkai, What kind of "soft materials" can we design from molecular gels?, *Chem. – Asian J.*, 2011, **6**, 266–282.
11 A. R. Hirst and D. K. Smith, Solvent effects on supramolecular gel-phase materials: Two-component dendritic gel, *Langmuir*, 2004, **20**, 10851–10857.
12 A. R. Hirst, I. A. Coates, T. R. Boucheteau, J. F. Miravet, B. Escuder, V. Castelletto, I. W. Hamley and D. K. Smith, Low-molecular-weight gelators: Elucidating the principles of gelation based on gelator solubility and a cooperative self-assembly model, *J. Am. Chem. Soc.*, 2008, **130**, 9113–9121.
13 W. Edwards, C. A. Lagadec and D. K. Smith, Solvent-gelator interactions-using empirical solvent parameters to better understand the self-assembly of gel-phase materials, *Soft Matter*, 2011, **7**, 110–117.
14 J. Chen, J. W. Kampf and A. J. McNeil, Comparing molecular gelators and nongelators based on solubilities and solid-state interactions, *Langmuir*, 2010, **26**, 13076–13080.
15 M. L. Muro-Small, J. Chen and A. J. McNeil, Dissolution parameters reveal role of structure and solvent in molecular gelation, *Langmuir*, 2011, **27**, 13248–13253.
16 M. Raynal and L. Bouteiller, Organogel formation rationalized by Hansen solubility parameters, *Chem. Commun.*, 2011, **47**, 8271–8273.
17 C. M. Hansen, *Hansen Solubility Parameters: A User's Handbook*, CRC Press, Boca Raton, Fla., 2000.
18 C. M. Hansen, 50 Years with solubility parameters – past and future, *Prog. Org. Coat.*, 2004, **51**, 77–84.
19 J. Gao, S. Wu and M. A. Rogers, Harnessing Hansen solubility parameters to predict organogel formation, *J. Mater. Chem.*, 2012, **22**, 12651–12658.
20 H. Q. Xu, J. Song, T. Tian and R. X. Feng, Estimation of organogel formation and influence of solvent viscosity and molecular size on gel properties and aggregate structures, *Soft Matter*, 2012, **8**, 3478–3486.
21 S. J. Liu, W. Yu and C. X. Zhou, Solvents effects in the formation and viscoelasticity of DBS organogels, *Soft Matter*, 2013, **9**, 864–874.
22 N. Yan, Z. Y. Xu, K. K. Diehn, S. R. Raghavan, Y. Fang and R. G. Weiss, Pyrenyl-linker-glucono gelators. Correlations of gel properties with gelator structures and characterization of solvent effects, *Langmuir*, 2013, **29**, 793–805.
23 N. Yan, Z. Xu, K. K. Diehn, S. R. Raghavan, Y. Fang and R. G. Weiss, How do liquid mixtures solubilize insoluble gelators? Self-assembly properties of pyrenyl-linker-glucono gelators in tetrahydrofuran-water mixtures, *J. Am. Chem. Soc.*, 2013, **135**, 8989–8999.
24 S. Yamasaki and H. Tsutsumi, Microscopic studies of 1,3-2,4-di-*O*-benzylidene-D-sorbitol in ethylene glycol, *Bull. Chem. Soc. Jpn.*, 1994, **67**, 906–911.
25 J. M. Smith and D. E. Katsoulis, Gelation of silicone fluids using 1,3/2,4-dibenzylidene sorbitol, *J. Mater. Chem.*, 1995, **5**, 1899–1903.
26 S. Yamasaki and H. Tsutsumi, The dependence of the polarity of solvents on 1,3/2,4-di-*O*-benzylidene-D-sorbitol gel, *Bull. Chem. Soc. Jpn.*, 1995, **68**, 123–127.
27 D. J. Mercurio, S. A. Khan and R. J. Spontak, Dynamic rheological behavior of DBS-induced poly(propylene glycol) physical gels, *Rheol. Acta*, 2001, **40**, 30–38.
28 W. Frassdorf, M. Fahrlander, K. Fuchs and C. Friedrich, Thermorheological properties of self-assembled dibenzylidene sorbitol structures in various polymer matrices: Determination and prediction of characteristic temperatures, *J. Rheol.*, 2003, **47**, 1445–1454.
29 E. A. Wilder, C. K. Hall, S. A. Khan and R. J. Spontak, Effects of composition and matrix polarity on network development in organogels of poly(ethylene glycol) and dibenzylidene sorbitol, *Langmuir*, 2003, **19**, 6004–6013.

30 M. Dumitras and C. Friedrich, Network formation and elasticity evolution in dibenzylidene sorbitol/poly-(propylene oxide) physical gels, *J. Rheol.*, 2004, **48**, 1135–1146.

31 D. L. VanderHart, J. F. Douglas, S. D. Hudson, J. M. Antonucci and E. A. Wilder, NMR characterization of the formation kinetics and structure of di-*O*-benzylidene sorbitol gels self-assembled in organic solvents, *Langmuir*, 2011, **27**, 1745–1757.

32 S. R. Raghavan and B. H. Cipriano, Gel formation: Phase diagrams using tabletop rheology and calorimetry, in *Molecular Gels*, ed. R. G. Weiss and P. Terech, Springer, Dordrecht, 2005, pp. 233–244.

33 X. Huang, P. Terech, S. R. Raghavan and R. G. Weiss, Kinetics of 5 alpha-cholestan-3 beta,6-yl *N*-(2-naphthyl)-carbamate/*n*-alkane organogel formation and its influence on the fibrillar networks, *J. Am. Chem. Soc.*, 2005, **127**, 4336–4344.

Electronic Supplementary Material (ESI) for Soft Matter.

Supporting Information for:

Insights into Organogelation and its Kinetics from Hansen Solubility Parameters. Toward *a priori* Predictions of Molecular Gelation.

Kevin K. Diehn, Hyuntaek Oh, Reza Hashemipour, Richard G. Weiss and Srinivasa R. Raghavan

Contents:

I. Experimental Section:

Materials. DBS (1,3:2,4-divinylbenzylidene sorbitol) was obtained from Milliken Chemicals. Solvents were acquired from Sigma-Aldrich and TCI America and used without further purification.

Preparation of DBS Gels. DBS was added to solvents at desired weight-by-volume percent. Samples were heated to 125°C until a transparent sol was obtained. For solvents with boiling points near or below 125°C, airtight, high pressure vials from Ace Glass Inc. (Vineland, NJ, USA) were used to prevent evaporation of the sample. If samples could not be dissolved, they were classified as insoluble. Samples were cooled with running water (22°C) for 90 seconds until they reached room temperature. They were then placed on the countertop for further observation. The classification scheme is further described in the main text.

Rheological Studies. Dynamic rheological experiments were performed on an AR2000 stress-controlled rheometer (TA Instruments). Samples were run on a parallel-plate geometry (25 mm plate, 0.5 mm gap). Dynamic frequency spectra were obtained in the linear viscoelastic regime of each sample, as determined by dynamic strain-sweep experiments

II. Description of Fitting Procedures and Algorithm:

In order to visualize the regions of DBS outcomes, each solvent point is plotted in 3-D Hansen space, where each axis represents one of the HSPs (δ_D, δ_P, δ_H). The solvent points are color-coded based on the outcome of the sample (Soluble, **S** = blue; Slow Gel, **SG** = green; Instant Gel, **IG** = red; Insoluble, **I** = yellow). Next, spheres are drawn around these regions in 3-D space as prescribed by Hansen for polymer solubility studies. The spheres are defined by their center point ($\delta_{Dcenter}$, $\delta_{Pcenter}$, $\delta_{Hcenter}$) and their radius R. To determine the best placement and size of the sphere, the sphere must be drawn such that "good" solvent points lie inside it and "bad" solvent points are excluded from it. We start with the sphere for the sol (**S**) region. In this case, soluble points should be inside the **S** sphere and all other points should be outside. A desirability function is used to determine the goodness-of-fit for a given radius and center point of the sphere. The desirability function (DF) is defined as:

$$\text{Desirability Function (DF)} = \left(A_1 \times A_2 \times \ldots A_n\right)^{\frac{1}{n}}$$

$$\text{where } A_i = \begin{cases} 1 & \text{for good solvent inside sphere} \\ 1 & \text{for bad solvent outside sphere} \\ e^{-|R_i - R_S|} & \text{for all other cases} \end{cases}$$

where R_i is the distance in 3-D Hansen space from the solvent point i to the center of the **S** sphere and R_S is the radius of the **S** sphere. n is the total number of solvent points.

II. Description of Fitting Procedures and Algorithm (cont'd):

We use an algorithm based on Hansen's work in which the center of the **S** sphere is guessed based upon the soluble points, the optimal value of the radius R_S is determined via value of the DF, and the process is repeated for nearby values of the center point. The initial guess for the center of the **S** sphere is based on the average HSP of each of the solvents in which DBS is soluble. With this initial center point, the radius R_S of this sphere is varied from very small values ($R_{S,min} = 1$) to very large values ($R_{S,max} = 25$). Based on the DF value at each of these radii, the optimal radius is selected.

Next, a cube (usually of side length $L = 1$) is drawn around the initial guess of the center point. For each corner of the cube, the optimal value of the sphere radius is determined by varying the radius and calculating the value of the DF. From these nine points (eight points at the cube corners and one point in the cube center), the point with the highest value of the DF is selected. If the point with the highest DF is the cube center, the algorithm repeats the cube iteration with a cube of a smaller length ($L= 0.5$, then $L = 0.3$) until the best center and radius combination is determined. If the point with the highest DF is one of the cube corners, the cube iteration is repeated. Ultimately, we determine the combination of center point and radius R_S that maximizes the DF. This fixes the solubility **S** sphere.

For the remaining 3 outcomes (**SG**, **IG** and **I**), the center point of the corresponding spheres is fixed to be identical to that of the **S** sphere (see main text). The iteration is then done only to optimize the radii of these spheres. It should be noted that our analysis procedure is general enough and can account for each outcome having distinct sphere centers as well as radii. The MATLAB program written for this study allows the user to choose between the two options.

III. Table S1. Solvents tested and DBS sample outcomes in these solvents

Species	Abbr.	δ_P	δ_H	$2\delta_D$	1 wt% DBS	5 wt% DBS	10 wt% DBS
Acetone	ACT	10.40	7.00	31.00	S	IG	IG
Triethyl phosphate	TEP	11.40	9.20	33.40	S	SG	IG
Cyclopentanone	CPN	11.90	5.20	35.80	S	SG	IG
N-methyl-2-pyrrolidone	NMP	12.30	7.20	36.00	S	S	S
Chloroacetonitrile	CAN	13.60	2.00	34.80	S	IG	IG
Dimethyl formamide	DMF	13.70	11.30	34.80	S	S	S
Caprolactone (epsilon)	CAP	15.00	7.40	39.40	S	SG	SG
Dimethyl sulfoxide	DMSO	16.40	10.20	36.80	S	S	S
2-pyrrolidone	PYR	17.40	11.30	38.80	S	S	S
Ethylene glycol butyl ether	EGBE	5.10	12.30	32.00	SG	IG	IG
Diethylene glycol butyl ether	dEGBE	7.00	10.60	32.00	SG	IG	IG
Cyclopentanol	CPOH	7.60	15.60	36.20	SG	IG	IG
Acetophenone	ATP	8.60	3.70	39.20	SG	IG	IG
Diethylene glycol ethyl ether	dEGEE	9.20	12.20	32.20	SG	IG	IG
Ethylene glycol ethyl ether	EGEE	9.20	14.30	32.40	SG	IG	IG
Dimethyl phthalate	DMPH	10.80	4.90	33.20	SG	IG	IG
Ethylene Glycol	EG	11.00	26.00	34.00	SG	IG	I
Methanol	MOH	12.30	22.30	30.20	SG	IG	IG
Triethylene glycol	TEG	12.50	18.60	32.00	SG	SG	IG
Hydroxyethyl acrylate	HEA	13.20	13.40	32.00	SG	IG	IG
Propionitrile	PPN	14.30	5.50	30.60	SG	IG	IG
Acetonitrile	ATN	18.00	6.10	30.60	SG	IG	IG
Xylene	XYL	1.00	3.10	35.20	IG	I	I
Toluene	TOL	1.40	2.00	36.00	IG	I	I
1-decanol	DOH	2.60	10.00	35.00	IG	I	I
1-octanol	OOH	3.30	11.90	34.00	IG	I	I
1-butanol	BOH	5.70	15.90	32.00	IG	I	I
n-butyl methacrylate	BMA	6.40	6.60	31.20	IG	I	I
Methyl methacrylate	MMA	6.50	5.40	31.60	IG	I	I
1-propanol	POH	6.80	17.40	32.00	IG	I	I
Isooctanol	iOOH	7.30	12.90	28.80	IG	IG	I
Ethanol	EOH	8.80	19.40	31.60	IG	IG	I
Nitromethane	NM	18.80	5.10	31.60	IG	IG	I
Decane	DEC	0	0	31.4	I	I	I

Figure S1. Overview of MATLAB HSP 3D Plotting and Fitting Program

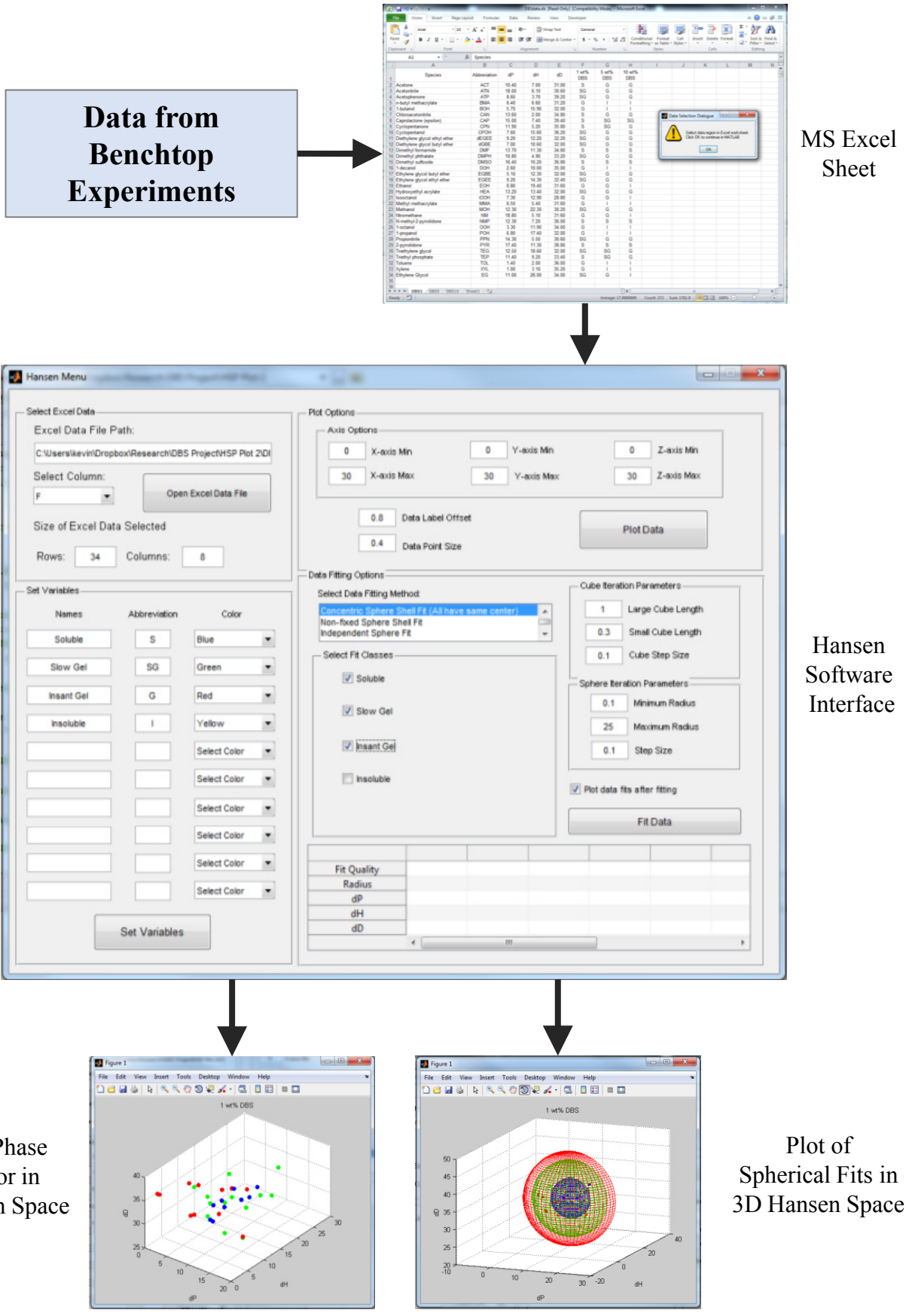

Figure S2 (a). Enlarged version of the 3D plot for 1% DBS. This is the same as Figure 2a in the main text. The larger size allows the individual solvent points to be seen. Abbreviations correspond to those in Table S1.

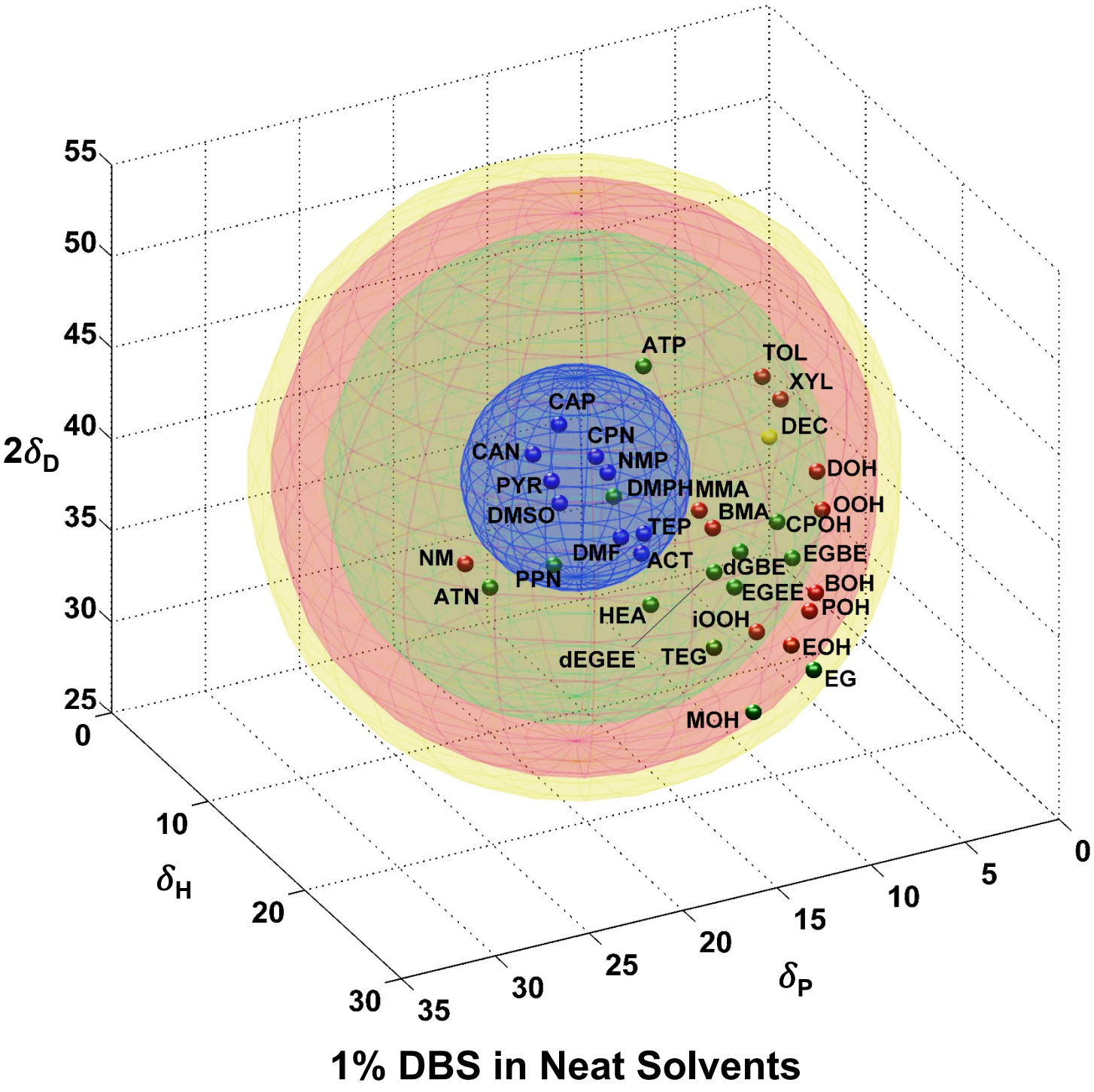

Figure S2 (b). Enlarged version of the 3D plot for 5% DBS. This is the same as Figure 2b in the main text. The larger size allows the individual solvent points to be seen. Abbreviations correspond to those in Table S1.

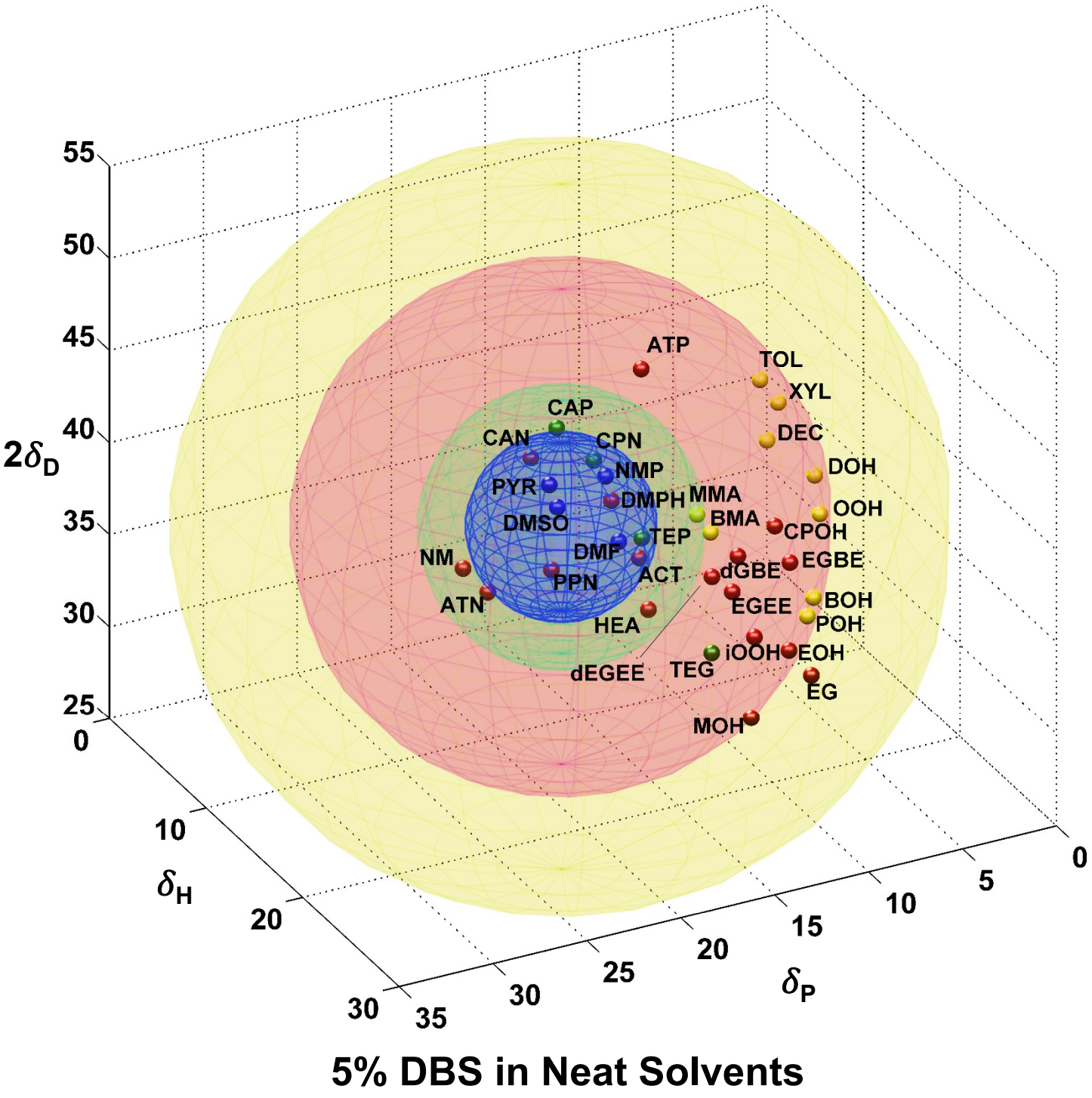

5% DBS in Neat Solvents

Figure S2 (c). Enlarged version of the 3D plot for 10% DBS. This is the same as Figure 2c in the main text. The larger size allows the individual solvent points to be seen. Abbreviations correspond to those in Table S1.

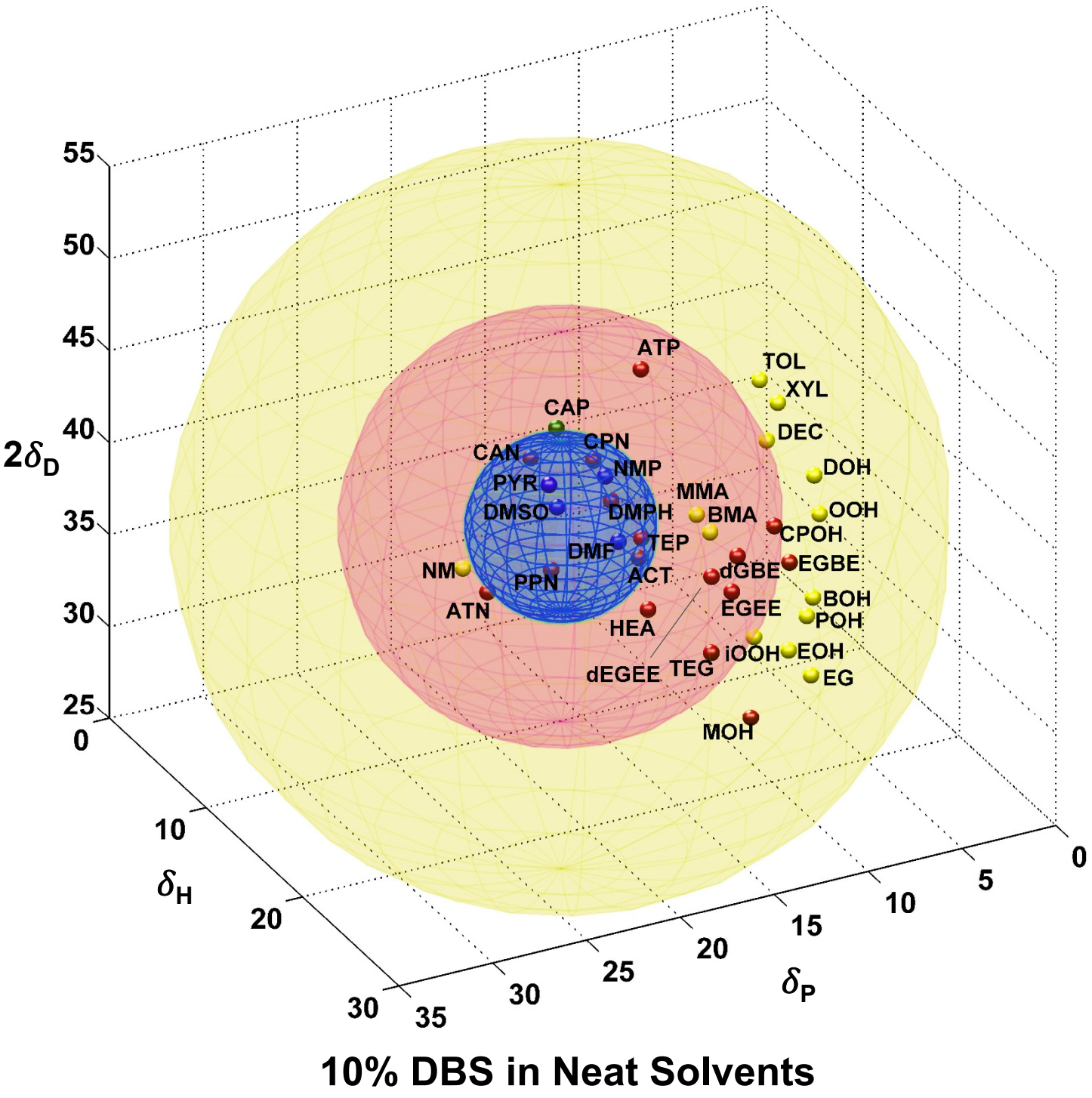

10% DBS in Neat Solvents

Figure S3. Correlation of gel modulus with Hansen parameters: Comparing various options. Plots of *G*' for 5% DBS gels are shown against differences in the individual Hansen solubility parameters (δ_D, δ_P, δ_H). This is compared with the plot of *G*' vs. R_0, which was presented in Figure 3 in the main text.

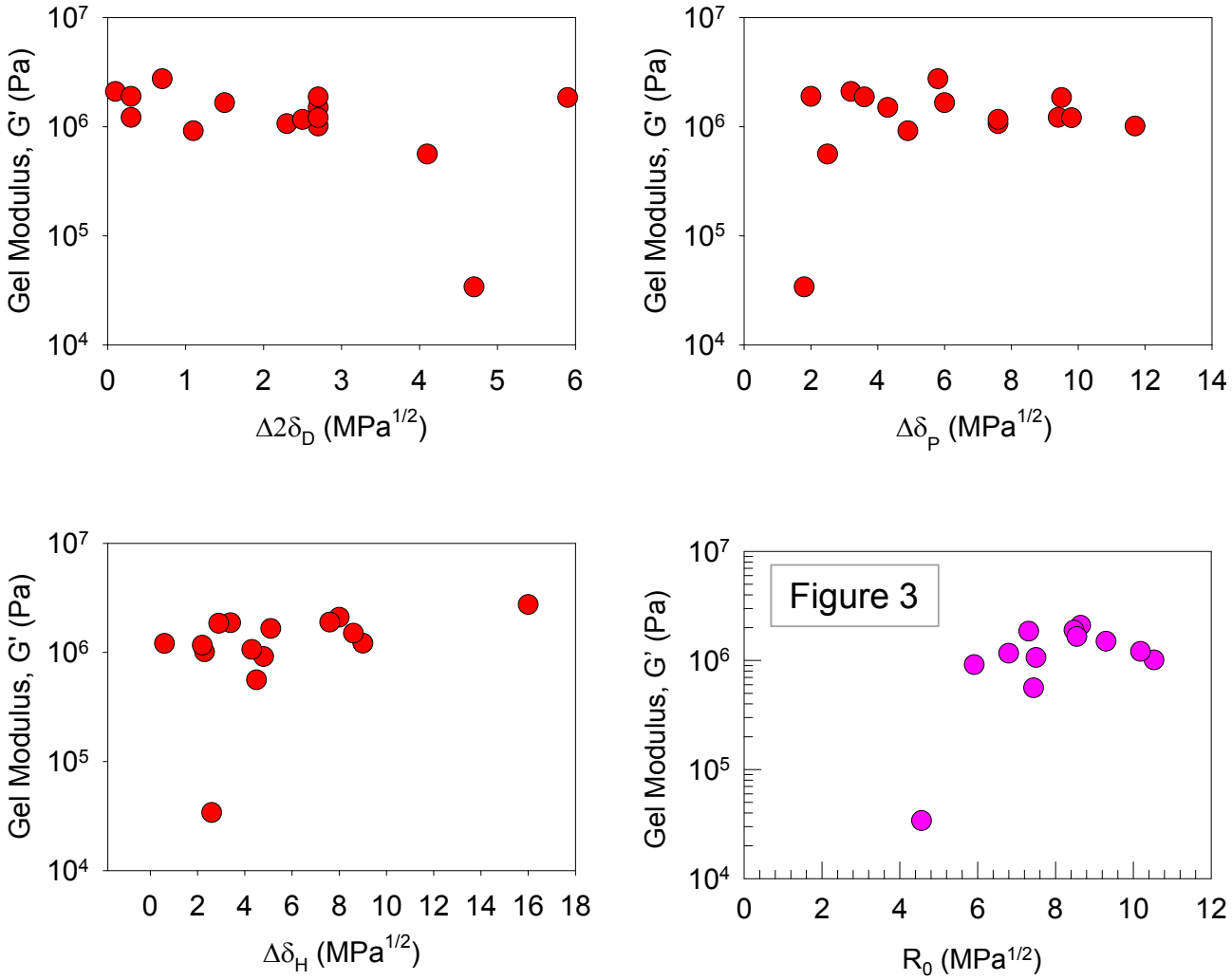

Figure S4. Outcomes for DBS in blends of various solvents with DMSO: Top view. This is a different view (projection onto the δ_P- δ_H plane) of the data that was presented in Figure 5. The data correspond to 5% DBS in mixtures of DMSO and the following solvents: toluene (TOL), decanol (DOH), octanol (OOH), butanol (BOH) and ethylene glycol (EG). the pure DMSO point is near the center of the solubility (**S**) sphere (in blue). For the mixtures, the sample outcomes are color coded as: sols (**S**, blue), slow gels (**SG**, green), instant gels (**IG**, red) and insoluble (**I**, yellow).

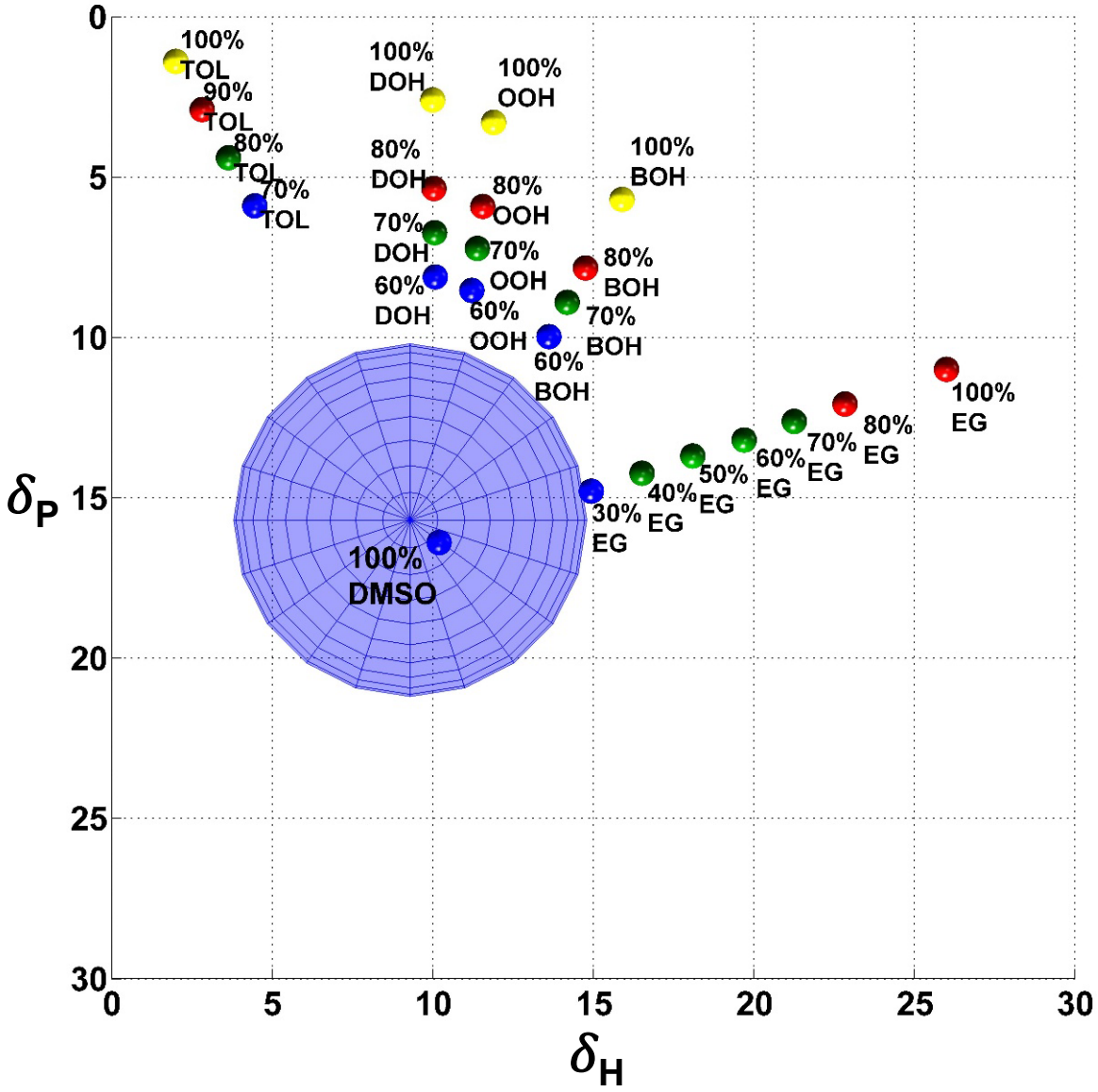

Figure S5. Predicted behavior of DBS in blends of two solvents in which it is insoluble. As an example, for the case of 10% DBS, we consider nitromethane (NM) and 1-octanol (OOH) as two solvents in which it is insoluble. As seen below, the two solvents occur on either side of the solubility (S) sphere. Thus, a line drawn between the solvents is expected to pass through all the 4 regions, i.e., sol (**S**, blue), slow gels (**SG**, green), instant gels (**IG**, red) and insoluble (**I**, yellow), depending on the ratios of the solvents.